The following publication W. Wang et al., "Optical Single Sideband Signal Reconstruction Based on Time-Domain Iteration," in Journal of Lightwave Technology, vol. 39, no. 8, pp. 2319-2326, 15 April 2021 is available at https://doi.org/10.1109/JLT.2021.3050855.

Optical Single Sideband Signal Reconstruction Based on Time-Domain Iteration

Wei Wang, Dongdong Zou, Zibin Li, Qi Sui, Zizheng Cao, Chao Lu, Fan Li and Zhaohui Li

***Abstract*—Due to its low cost, simple architecture and robustness to fiber dispersion, single sideband (SSB) transmission with direct detection (DD) system is an attractive solution for 80-km inter data center interconnects (DCIs). However, it will suffer performance penalty caused by the signal-to-signal beating interference (SSBI). Kramers-Kronig (KK) receiver has been extensively investigated for SSBI elimination by reconstructing the SSB signal. The nonlinear operations in KK algorithm require up-sampling to cope with spectral broadening, which results in high complexity for practical application. Optical signal phase retrieval method based on the minimum phase signal has also been investigated for SSB signal recovery, in which the SSB and DC-Value properties are iteratively imposed on the amplitude signal in frequency domain. In this paper, we propose a low complexity iterative algorithm for minimum phase signal recovery without up-sampling in time domain. Finite impulse response (FIR) filter is applied to iteratively generate the SSB signal and update the phase component. Based on the proposed scheme, the transmission of 30GHz SSB 16-QAM discrete multitone (DMT) signal over 80km single mode fiber (SMF) is successfully demonstrated with the bit error rate (BER) below the hard-decision forward error correction (HD-FEC) threshold of 3.8×10^{-3}. The experimental results show that, the BER performance of KK scheme with up-sampling factor of 2, frequency-domain iterative scheme and our proposed scheme is almost the same. However, compared with the KK scheme, the proposed method can save the numbers of adders and multipliers by the factors of 29 and 7, while the factors are 5.5 and 4 comparing to the frequency-domain iteration scheme.**

***Index Terms*—Signal-to-signal beating interference (SSBI), phase retrieval, minimum phase signal, finite impulse response (FIR) filter.**

Manuscript received XXX XXXX; revised XXX, XXXX; accepted XXX, XXXX. This work is partly supported by the National Key R&D Program of China (2019YFA0706300); Local Innovation and Research Teams Project of Guangdong Pearl River Talents Program (2017BT01X121); Pearl River S&T Nova Program of Guangzhou (201710010051, 2018B010114002); National Natural Science Foundation of China under Grants 61871408, Sichuan Science and Technology Program (2020YFH0108). (*W. Wang and D. Zou contribute equally to this paper, Corresponding Author: Fan Li*)

W. Wang, D. Zou, Z. Li and F. Li are with the Key Laboratory of Optoelectronic Materials and Technologies, School of Electronics and Information Technology, Sun Yat-Sen University, Guangzhou 510275, China (e-mail: lifan39@mail.sysu.edu.cn).

Q. Sui is with Southern Marine Science and Engineering Guangdong Laboratory (Zhuhai), Zhuhai, China (e-mail: suiqi@sml-zhuhai.cn).

Zizheng Cao is with the Institute for Photonic Integration, Eindhoven University of Technology, 5600MB Eindhoven, The Netherlands (e-mail: z.cao@tue.nl).

C. Lu is with the Department of Electronic and Information Engineering, Hong Kong Polytechnic University, Kowloon, Hong Kong and he is also with the Key Laboratory of Optoelectronic Materials and Technologies, School of Electronics and Information Technology, Sun Yat-Sen University, Guangzhou 510275, China (e-mail: enluchao@polyu.edu.hk).

Z. Li is the Key Laboratory of Optoelectronic Materials and Technologies, School of Electronics and Information Technology, Sun Yat-Sen University, Guangzhou 510275, China, and he is also with Southern Laboratory of Ocean Science and Engineering (Guangdong, Zhuhai), Zhuhai, 519000, China (e-mail: lzhh88@mail.sysu.edu.cn).

I. Introduction

Recently, driven by the emerging broadband applications such as cloud computing, video conferencing, virtual reality and augmented reality (VR/AR), large-capacity optical transmission system with low cost and simple architecture is extremely desired for data center interconnects (DCIs). Since the distance of inter-DCIs will reach 80km in the near future, the research of beyond 100Gb/s signal transmission over 80km single mode fiber (SMF) based on direct detection (DD) has been drawn much attention [1]. Due to the low cost, power consumption and system complexity, intensity modulation and direct detection (IM/DD) system is considered as a promising candidate for short reach optical interconnects applications [2-3]. However, double sideband (DSB) signal will suffer serious frequency selected power fading caused by chromatic dispersion (CD) in conventional IM/DD system, which limits the transmission capacity and distance of the system and can hardly satisfy the transmission requirement of inter-DCIs [4-5].

Since single sideband (SSB) signal is more robust to fiber dispersion, SSB method in DD system has been extensively studied [6-8]. However, signal-to-signal beating interference (SSBI) is the major obstacle in SSB DD systems due to the square law-detection of a single-ended photodiode (PD). This interference will deteriorate the system performance, especially at low carrier-to-signal power ratio (CSPR). Several linearization techniques are proposed to eliminate SSBI, such as beat interference cancellation balanced receiver (BICBR) [9], digital iteration SSBI estimation and cancellation [10-11], and iterative linearization filter [12]. Recently, Kramers-Kronig (KK) receiver is proposed to avoid SSBI by reconstructing the SSB signal [13-18]. Since the phase and intensity of the SSB signal meeting the minimum phase condition (MPC) are related by the Hilbert transform, the phase component can be recovered from the received intensity [13], [19-20]. However, the major obstacle of KK receiver for practical application is the high computational complexity. The nonlinear operations such as logarithmic and exponential operations in KK algorithm leads to spectral broadening, thus up-sampling is required before KK operation. In the past few decades, Gerchberg-Saxton (G-S) algorithm is proposed to recover the

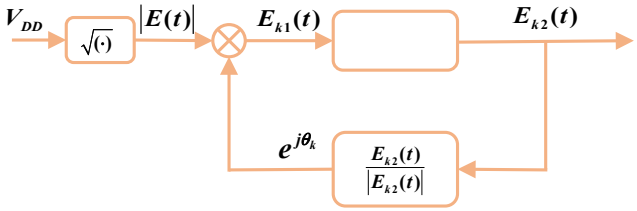

Fig. 1. Schematic diagram of time-domain iteration method for SSB signal reconstruction.

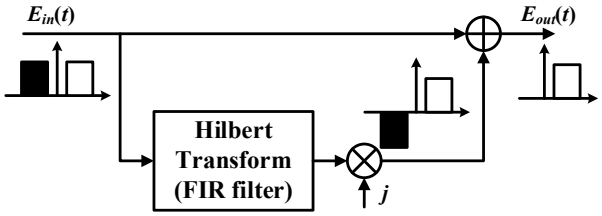

Fig. 2. Schematic of digital discrete Hilbert transform filter for SSB signal generation.

phase in image processing. It is realized by iteratively imposing the constraint conditions in both space and Fourier domains [21]. A modified G-S algorithm based on multiple distinct dispersion elements and intensity measurements has been investigated in DD system using phase retrieval [22]. Recently, R. K. Patel et al. develop a frequency-domain iterative method for optical phase retrieval based on the SSB and DC-Value property of the minimum phase signal with simulation [23]. Since the iteration method avoids the nonlinear operations, up-sampling is not required compared to KK receiver. However, the iterative process in Ref. [23] is realized in frequency domain, fast Fourier transform and inverse fast Fourier transform (FFT/IFFT) pairs are required in each iteration.

In this paper, a low complexity iterative algorithm is proposed for optical SSB signal reconstruction in time domain. Based on the SSB and DC-Value property of the minimum phase signal, finite impulse response (FIR) filter is implemented to iteratively recover the SSB signal. The proposed method is also free from up-sampling as the nonlinear operations are avoided. Although the SSBI iteration cancellation (IC) method in Refs. [10-12] is also realized by time-domain iteration, SSBI is iteratively estimated by using square law of the recovered SSB signal, and then subtracted from the directly-detected signal to remove the SSBI sufficiently. As for our proposed time-domain iterative method, the iterative process is used to generate SSB signal and update the phase component. In order to verify the effectiveness of the proposed method in eliminating SSBI, the transmission of a 30GHz SSB 16-QAM discrete multitone (DMT) signal over 80km SMF is experimentally demonstrated. The experimental results show that, our proposed scheme can achieve the same bit error rate (BER) performance as the frequency-domain iterative method and KK scheme with up-sampling factor of 2. Compared to frequency-domain iterative method, the FFT/IFFT pairs in each iteration for time-frequency domain conversion can be saved in our proposed scheme. As discussed for computational complexity in detail, the proposed method can save the numbers of adders and multipliers by the factors of 29 and 7 compared with the KK scheme, while comparing with the frequency-domain iterative algorithm, the factors of 5.5 and 4 for adders and multipliers are achieved, respectively.

The rest of the article is organized as follows: Section II presents the principle of the time-domain iterative method and the structure of FIR filter. In Section III, the experimental setup and results of 30GHz SSB 16-QAM DMT signal transmission are described and discussed. Section IV analyzes the computational complexity of these two iterative methods. Finally, conclusions are drawn in Section V.

II. Theory

In this section, we introduce the principle of the proposed phase retrieval method based on time-domain iteration at first. Then, the structure of the FIR filter for SSB signal generation is given, and the possibility for computational complexity reduction is discussed.

A. Principle of the time-domain iteration method

In SSB DD system, the optical SSB signal can be expressed as:

$$E(t) = E_c + E_s(t), \tag{1}$$

where E_c represents the optical carrier, and $E_s(t)$ is the complex SSB signal. $E_c > |E_s(t)|$ ensures the minimum phase condition. At the receiver side, a single PD is used to detect the signal, and the received signal can be written as:

$$V_{DD} = |E_c|^2 + |E_s(t)|^2 + 2\,\mathrm{Re}\{E_c \cdot E_s(t)\}, \tag{2}$$

The first and second terms on the right side of equation (2) are the DC component and SSBI, respectively. $2\,\mathrm{Re}\{E_c \cdot E_s(t)\}$ is our desired signal, and $\mathrm{Re}\{\cdot\}$ denotes taking the real part operation. Figure 1 describes the schematic diagram of the time-domain iterative method for SSB signal reconstruction. The amplitude of the optical SSB signal can be obtained by square root operation as:

$$|E(t)| = \sqrt{V_{DD}}. \tag{3}$$

Then, the real amplitude $|E(t)|$ is multiplied with the complex phase component $e^{j\theta_k}$, in which the phase θ_k is initialized to zero and updated iteratively from the generated SSB signal. Then, a complex signal $E_{k1}(t)$ is obtained. After that, the SSB and DC value properties of the minimum phase signal are adopted, which is achieved by FIR filter. The structure of the FIR filter will be introduced in Section II-B. An SSB signal $E_{k2}(t)$ is generated after the FIR filter, and the frequency response of $E_{k2}(t)$ can be expressed as:

$$\tilde{E}_{k2}(\omega) = \begin{cases} p\tilde{E}_{k1}(\omega), & \omega > 0 \\ \tilde{E}_{k1}(\omega), & \omega = 0 \\ 0, & \omega < 0 \end{cases}, \tag{4}$$

where $\tilde{E}_{k1}(\omega)$ is the frequency response of $E_{k1}(t)$ and $\tilde{E}_{k2}(0) = E_c$. Since the PD utilized in our experiment is

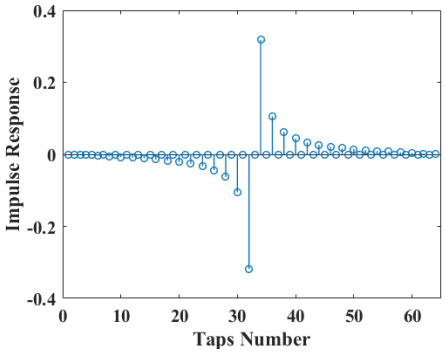

Fig. 3. Impulse response of the FIR filter with 64-taps in time domain.

AC-coupled, the DC component is lost after optical to electrical conversion. Thus, a digital carrier is added at the receiver side for minimum phase signal reconstruction. The magnitude of the carrier amplitude is calculated according to the CSPR of the optical SSB signal, which is defined as:

$$CSPR(dB) = 10\log_{10}(|E_c|^2 / |E_s(t)|^2). \tag{5}$$

According to equation (4), the tap coefficients should be multiplied with a scaling factor p, which is given by:

$$p = \begin{cases} 2, & k = 1 \\ 1, & k > 1 \end{cases}, \tag{6}$$

where k represents the iteration number. As described in [23], the real and imaginary parts amplitude of the generated SSB signal are scaled by a factor of 0.5 in first iteration. Thus, p=2 is implemented to adjust the amplitude of the SSB signal, and it can effectively speed up the convergence of the iterative process, which will be demonstrated in Section III. Then, the phase information can be calculated by:

$$e^{j\theta_k} = E_{k2}(t) / |E_{k2}(t)|. \tag{7}$$

And the updated phase component is used to obtain the complex signal $E_{k1}(t)$ as:

$$E_{k1}(t) = |E(t)| e^{j\theta_k}. \tag{8}$$

The minimum phase condition property is adopted in each iteration, and the convergence criteria is based on the mean squared error e_k between the $|E_{k2}(t)|$ and $|E(t)|$, which can be described as:

$$e_k = \frac{1}{N}\sum_{n=1}^{N} \left| |E_{k2}(n)| - |E(n)| \right|^2. \tag{9}$$

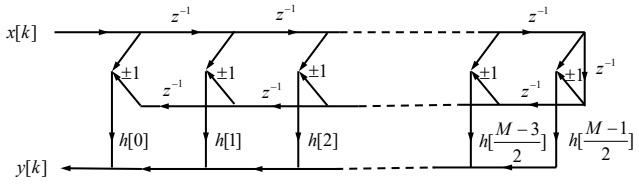

Fig. 4. Schematic diagram of the symmetric FIR filter.

The iterative process continues if the error e_k is greater than the threshold error e_h. In this paper, the number of iterations is adjusted until the error does not change significantly. It is considered to be converged, and the amplitude and phase of the generated SSB signal will be related by KK relation

B. Construction of FIR filter

Digital discrete Hilbert transform filter can be used for SSB signal generation [24-25]. Fig. 2 shows the schematic of digital discrete Hilbert transform filter for SSB signal generation. The frequency response of the Hilbert transform is described as:

$$H(\omega) = \begin{cases} e^{-j\pi/2}, & \omega > 0 \\ 0, & \omega = 0 \\ e^{j\pi/2}, & \omega < 0 \end{cases}, \tag{10}$$

where ω represents the angular frequency. And its impulse response in time domain can be expressed as:

$$h(t) = 1/\pi t. \tag{11}$$

As shown in Fig. 2, the input signal $E_{in}(t)$ is divided into two branches. The lower branch performs the Hilbert transform and multiplies with $e^{j\pi/2}$, thus all negative frequency components of the signal are phase-delayed by 180°. Afterwards, the output signal of the lower branch is added to the original signal $E_{in}(t)$, and an SSB signal $E_{out}(t)$ is generated.

However, the discrete Hilbert transform filter can be realized by N_h-taps FIR filter [26], and it can be modified as [24]:

$$h(n) = \begin{cases} \frac{2}{\pi n}\sin^2\left(\frac{\pi n}{2}\right), & n \neq 0 \\ 0, & n = 0 \end{cases}, \tag{12}$$

which can also be expressed as:

$$h(n) = \begin{cases} 0, & n \quad even \\ 2/\pi n, & n \quad odd \end{cases}. \tag{13}$$

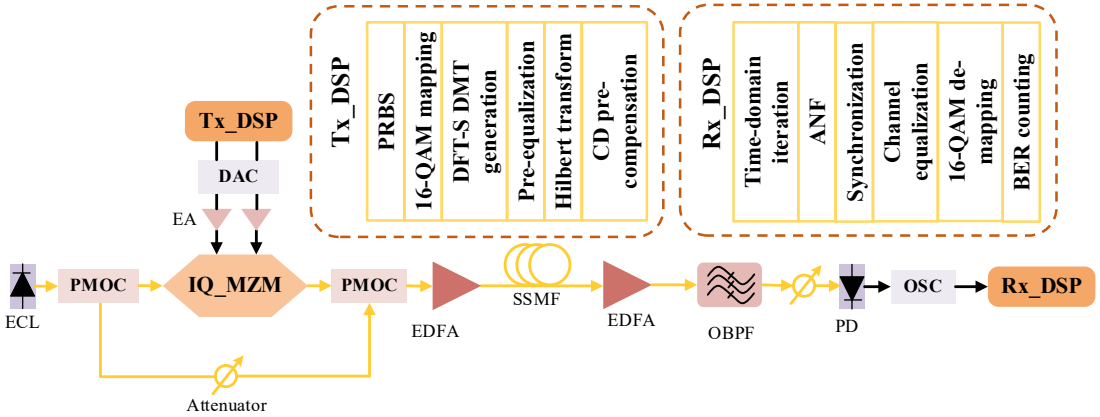

Fig. 5. Experimental setup and DSP block diagram of time-domain iteration scheme for 30GHz SSB 16-QAM DMT signal transmission and reception.

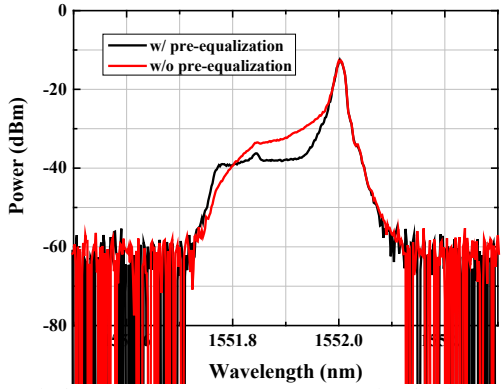

Fig. 6. Optical spectra of 30GHz SSB DMT signal with and without pre-equalization.

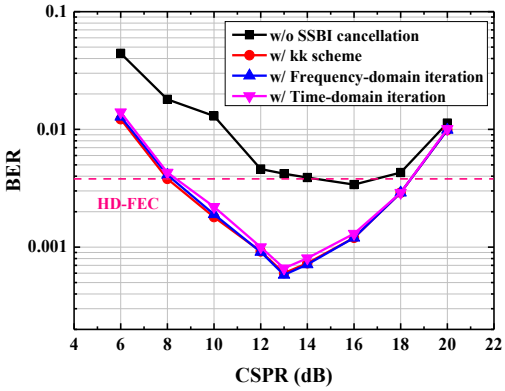

Fig. 8. BER performance versus CSPR of KK scheme, frequency-domain iterative scheme and time-domain iterative scheme.

According to equation (13), every even tap-coefficient is zero and can be ignored. It means that only half of the taps are valid. Fig. 3 gives the impulse response of the FIR filter with 64-taps. It shows that the structure of this FIR filter is symmetric, which means the number of the multipliers can be halved. Thus, the computational complexity is further reduced, and the schematic diagram of this symmetric FIR filter is shown in Fig. 4.

III. Experimental Setup and Results

The experimental setup and results of our proposed time-domain iterative method is described in this section. In order to verify the effectiveness of our proposed scheme for SSBI elimination, it is considered to compare with KK scheme and frequency-domain iterative scheme. The experimental results show that our proposed scheme can achieve almost the same performance with other two schemes.

A. Experimental setup

Figure 5 shows the experimental setup and digital signal processing (DSP) block diagram of our proposed scheme for 30GHz SSB 16-QAM DMT signal transmission and reception. At the transmitter, an optical carrier signal at 1550.004 nm emitting from an external cavity laser (ECL) is divided into two branches by a polarization maintaining optical coupler (PMOC). One is injected into the IQ modulator biased at null point for complex signal modulation. At the transmitter side DSP, the pseudo random bit sequence (PRBS) is mapped into 16-QAM symbols and then 30GHz discrete Fourier transform spread (DFT-S) DMT signal is generated. The FFT size is 1024, and the length of cyclic prefix (CP) is 32. Besides, 20 blocks of DMT symbols are inserted as training sequences (TSs). Then pre-equalization is applied to compensate the high frequency attenuation, and Hilbert transform is followed as it is a common method to generate SSB signal for both single-carrier and multi-carrier signals. In case of fiber transmission, electronic dispersion compensation (EDC) is applied for CD pre-compensation. The 30GHz SSB DMT signal is generated off-line in MATLAB and then uploaded into an 80 GSa/s sampling rate Fujitsu digital-to-analog converter (DAC) with 16GHz 3-dB bandwidth and 8-bit resolution. The real and imaginary part of SSB signal from two output ports of DAC are amplified by a 4-channel 32-Gbaud linear driver with 20-dB gain and then injected into the IQ modulator. The other branch is used for optical carrier coupling with the modulated signal by PMOC to obtain an optical SSB signal. The power and linewidth of the emitting optical carrier are 16 dBm and less than 100 kHz. The attenuator in lower branch is used to adjust the CSPR by varying the carrier power. Amplified by Erbium-doped fiber amplifier (EDFA), the optical SSB signal is then launched into

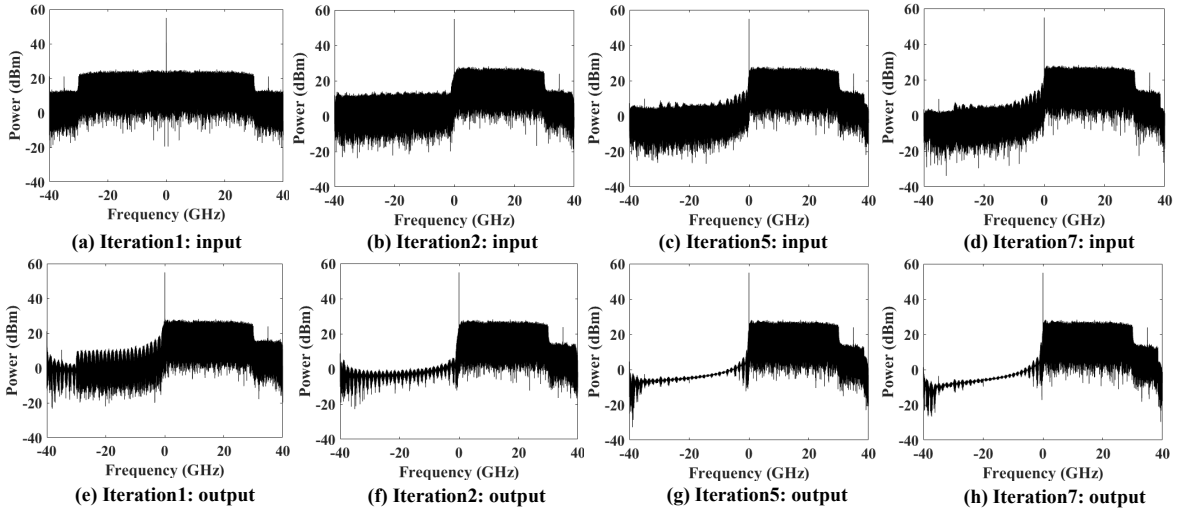

Fig. 7. Spectrum of the input signal $E_{k1}(t)$ and output signal $E_{k2}(t)$ in our proposed scheme after 1, 2, 5, and 7 iterations in BTB case with ROP and CSPR of -4dBm and 13dB.

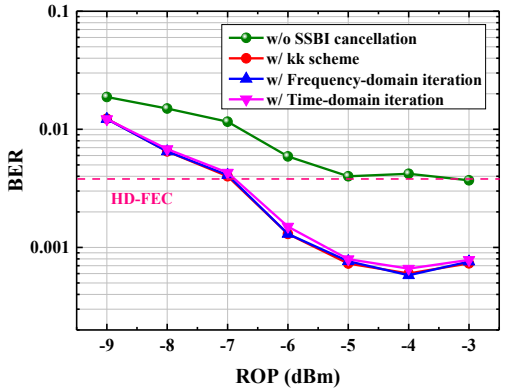

Fig. 9. BER performance versus ROP with CSPR of 13dB in BTB.

fiber. Another EDFA is applied to compensate the attenuation of fiber, and the optical bandpass filter (OBPF) is applied to filter out the noise. Fig. 6 shows the spectrum of 30GHz SSB DMT signal at the output of OBPF. It can be seen that, high frequency power attenuation is compensated with pre-equalization. Besides, the 20GHz narrowband interference can be clearly seen, which is from the leakage of the DAC.

At the receiver side, an attenuator is used to adjust the received optical power (ROP) and then the SSB signal is detected by a PIN PD with 3-dB bandwidth of 40GHz. Then, the received signal is captured by a Lecroy Oscilloscope (OSC) operating at 80 GSa/s sampling rate with 36GHz bandwidth. Finally, the captured samples are fed into off-line DSP for demodulation. Time-domain iteration is carried out first to recover the SSB signal. Then, an adaptive notch filter (ANF) is used to eliminate the clock leakage narrowband interference [27]. After synchronization, channel equalization is carried out

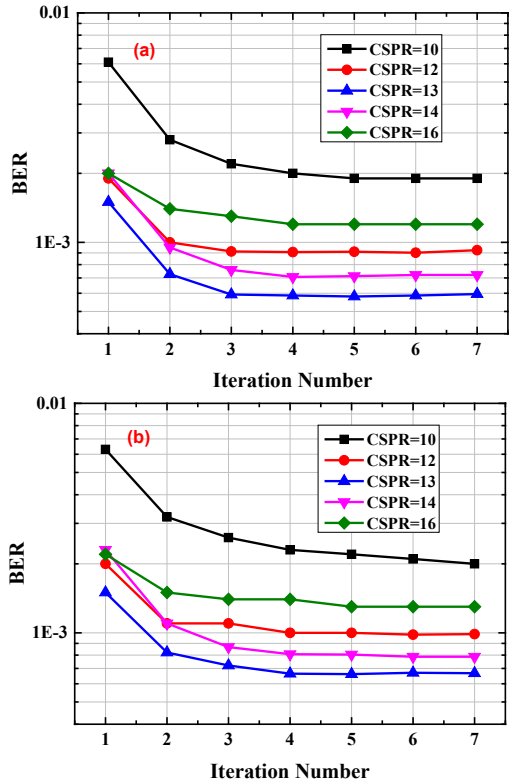

Fig. 10. BER performance versus the number of iterations for (a) frequency-domain iterative scheme and (b) time-domain iterative scheme.

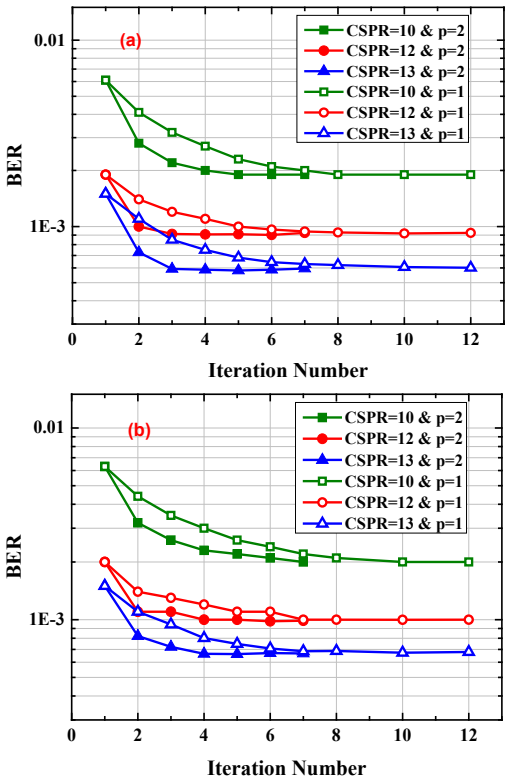

Fig. 11. BER performance versus the number of iterations with and without scaling factor p for (a) frequency-domain iterative scheme and (b) time-domain iterative scheme.

in frequency domain. Finally, 16-QAM de-mapping and BER counting are followed. Fig. 7 shows the spectrum of $E_{k1}(t)$ and $E_{k2}(t)$ after 1, 2, 5, 7 iterations in BTB with ROP and CSPR of -4dBm and 13dB. The accuracy of the signal reconstruction tends to converge after several iterations.

B. Optical back-to back performance analysis

The BER performance in BTB case is discussed first. The tap length of the FIR filter is set to be 21 in our test, and both two iteration schemes are carried out with 5 iterations. Fig. 8 compares the BER performance of KK scheme (up-sampling factor of 2), frequency-domain iterative scheme and our proposed scheme at -4dBm ROP. As shown in Fig. 8, the BER performance of these three schemes are almost the same. And the BER performance has been greatly improved compared with the case without SSBI cancellation, which means that our

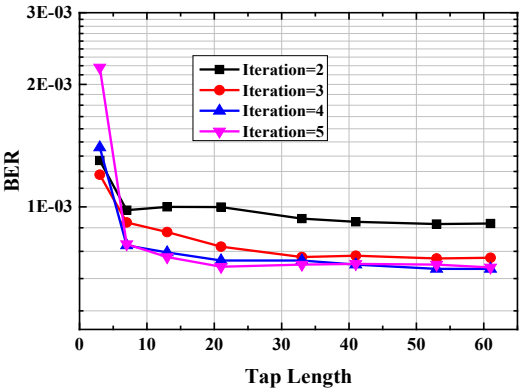

Fig. 12. BER performance versus tap length in BTB.

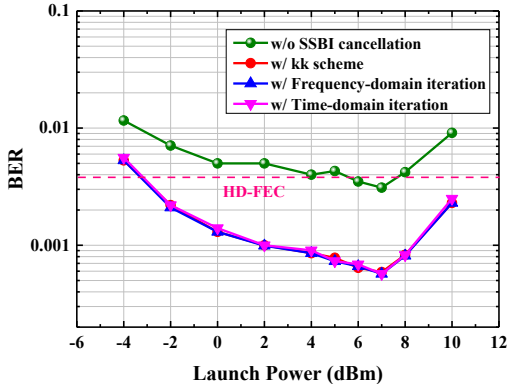

Fig. 13. BER performance versus launch power with CSPR of 13dB over 80km SMF transmission.

proposed scheme can effectively eliminate SSBI. And the optimal CSPR value in BTB is about 13dB. Since a high peak tone appears due to the clock leakage of the DAC in our experiment, and it falls within the signal bandwidth as shown in Fig. 6. This high peak tone will deteriorate the minimum phase condition, thus a lager carrier is required, which results in higher optimal CSPR value compared with the one in some references [11], [15]. Measured BER performance versus ROP with CSPR of 13dB is shown in Fig. 9, and we can find that the best ROP is -4dBm. Figs. 10(a) and 10(b) show the BER performance of frequency-domain iterative scheme and our proposed scheme under different iterations. The BER degrades with the increase of iterations and the improvement is not significant when the number of iterations reaches 5. Besides, the BER performance and convergence trend of these two iterative schemes are almost the same. Since the scaling factor p will influence the convergence process, the BER performance versus the number of iterations with and without scaling factor p is discussed in Fig. 11. More iterations are required when p=1 for both two iterative schemes. Thus, fewer iterations are required to achieve the best performance by utilizing scaling factor p. Finally, we also measure the BER performance under different tap lengths as shown in Fig. 12. However, increasing the number of taps cannot significantly improve the BER performance, and tap length of 21 is sufficient to converge.

C. 80km SMF transmission performance analysis

In our experiment, the length of fiber is fixed at 80km for fiber transmission test. The BER performance versus launch power with CSPR of 13dB is given in Fig. 13. BER degrades with the increase of the launch power. However, when the launch power is higher than 7dBm, the BER performance is getting worse due to the nonlinear effect of fiber. Since the BER curves of these three methods are nearly overlapping, they have the same optimal launch power of 7dBm. Fig. 14 shows the BER performance under different ROPs with CSPR and launch power of 13dB and 7dBm, respectively. And the optimal ROP is about -3dBm for 80km SMF transmission. The BER performance versus CSPR after 80km SMF transmission is shown in Fig. 15, and the launch power and ROP are 7dBm and -3dBm, respectively. As shown in Fig. 15, the optimal CSPR is about 13dB. Fig. 16 gives the BER performance versus tap length with CSPR of 13dB. And the constellations with 3-taps and 21-taps are inserted. The constellation with 21-taps is more convergence than the one of 3-taps. Finally, the BER performance under different iterations are also tested for both two iterative schemes over 80km SMF transmission as shown in Fig. 17, and 5 iterations are sufficient to reach convergence.

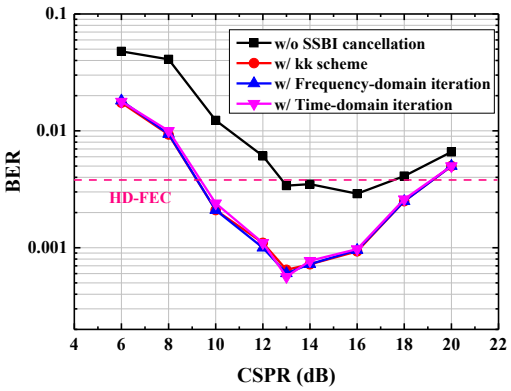

Fig. 15. BER performance versus CSPR after 80km SMF transmission.

IV. Computation Complexity Analysis

In this section, the computational complexity of these two iterative methods is analyzed and compared, and the complexity of KK scheme is also compared.

Assume that the sampling rate of the analog-to-digital converter (ADC) is f_s, which is much faster than the clock frequency f_{clock} of DSP chip. Therefore, parallel mechanism is often implemented in the DSP chip. The degree of

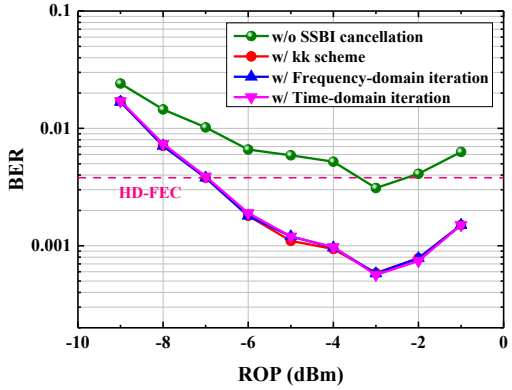

Fig. 14. BER performance versus ROPs with CSPR and launch power of 13dB and 7dBm over 80km SMF transmission.

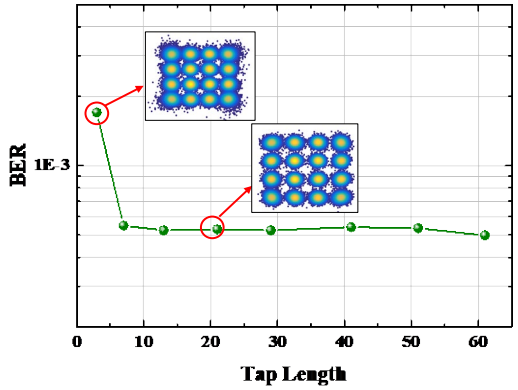

Fig. 16. BER performance versus tap length with CSPR of 13dB over 80km SMF transmission.

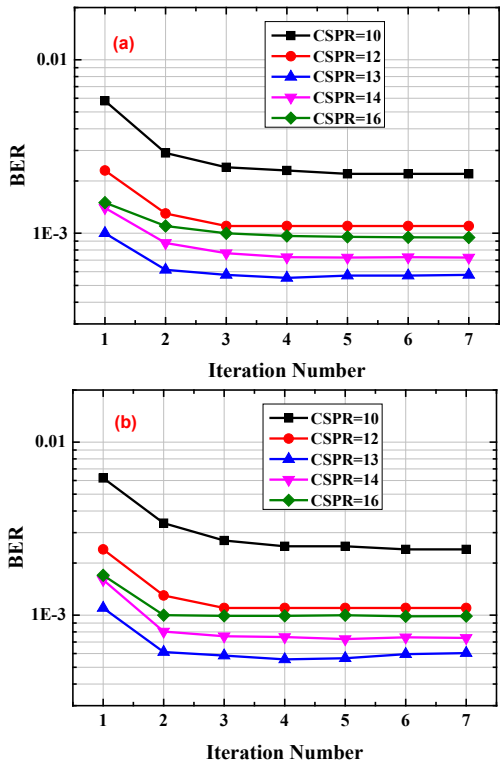

Fig. 17. BER performance versus the number of iterations over 80km SMF transmission for (a) frequency-domain iterative scheme and (b) time-domain iterative scheme.

parallelization is defined as $N = \lceil f_s / f_{clock} \rceil$, where $\lceil \cdot \rceil$ is the ceiling operator. In our previous work, the computational complexity of KK receiver has been discussed [28]. The complexity of the frequency-domain iterative scheme is also analyzed in [23]. Figs. 18(a) and 18(b) describe the DSP blocks for each parallelization of frequency-domain iterative scheme and time-domain iterative scheme, respectively. The nonlinear operators in these two DSP blocks can be achieved by look-up-table (LUT). Assume the vertical resolution of the ADC is 8 bits and the LUT is filled with 2-byte floating-point numbers, each LUT requires the memory size of $2^8 \times 2^4$ bits. Three LUTs are included in a parallel module for both two iterative schemes as shown in Fig. 18, which requires the memory size of 12kbits. For frequency-domain iterative

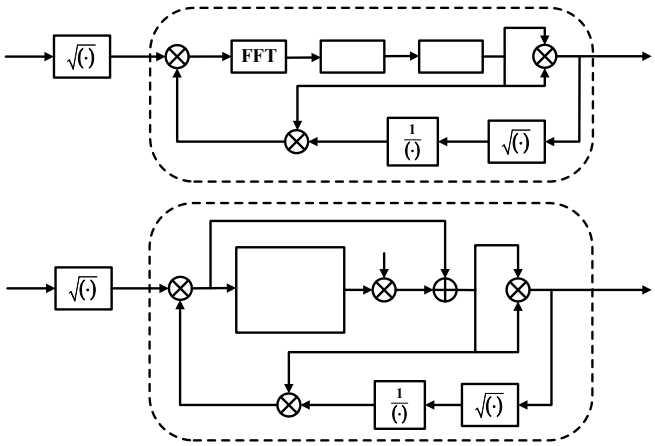

Fig. 18. DSP blocks for each parallelization of (a) frequency-domain iterative scheme and (b) time-domain iterative scheme.

TABLE I
REQUIRED HARDWARE RESOURCES

Scheme	Number of adders	Number of multipliers	Memory size (kbit)
KK scheme	$(3N_s+N_h/2)RN$	$(3(N_s+1)+N_h/2+2)RN$	$16RN$
Frequency-domain iterative scheme	$(N+6N\log_2 N)k$	$(6N+4N\log_2 N)k$	$12N$
Time-domain iterative scheme	$(N_h+1)kN/2$	$(N_h+27)kN/4$	$12N$

scheme, the real value after square root operation is multiplied with the complex phase component, and $2N$ multipliers are required. After that, FFT/IFFT and MPC are followed. As discussed in Ref. [23], the scaling factor implementation can be realized by 1-bit shift operation. As for FFT operation, it includes $(N\log_2 N)/2$ complex multiplications and $N\log_2 N$ additions. And one complex multiplication requires 4 real multipliers and 2 real adders, while one complex addition needs 2 real adders. Thus, a FFT operation including $2N\log_2 N$ real multipliers and $3N\log_2 N$ real adders, and the complexity of IFFT is the same as FFT. Square law $|(\cdot)|^2$, square root and inverse operation are followed to acquire the phase of the generated SSB signal. $2N$ multipliers and N adders are required for $|(\cdot)|^2$. As shown in Fig. 18, the division is replaced by a multiplication and an inverse realized by LUT. The stored $1/(\cdot)$ is multiplied with the complex signal $E_{k2}(t)$, and $2N$ multipliers are required. Thus, the total numbers of multipliers and adders for the frequency-domain iteration scheme can be calculated by $(2N+2\times 2N\log_2 N+2N+2N)k=(4N\log_2 N+6N)k$ and $(2\times 3N\log_2 N+N)k=(6N\log_2 N+N)k$, respectively.

Figure 18(b) gives the DSP blocks of time-domain iterative scheme. At first, the received signal is carried out by square root operation. Then the real value is multiplied with the complex phase component and $2N$ multipliers are required. N_h-taps FIR filter is applied to generate SSB signal. Since every even tap-coefficient is zero, only $(N_h-1)/2$ taps are valid (N_h is odd). Besides, the structure of the FIR filter is symmetric as shown in Fig. 4, and the multipliers can be halved. Thus, the numbers of multipliers and adders required in FIR filter are $(N_h-1)/4$ and $(N_h-3)/2$, respectively. In order to generate the SSB signal, a multiplication and an adder are followed after FIR filter. After that, phase information is calculated from the generated SSB signal, and $4N$ multipliers and N adders are needed in this process, which is the same as the frequency-domain iterative scheme. Therefore, the total numbers of multipliers and adders for the proposed scheme can be calculated by $(2N+(N_h-1)N/4+N+4N)k=(N_h+27)Nk/4$ and $((N_h-3)N/2+N+N)k=(N_h+1)Nk/2$.

Table I lists the numbers of real-valued multipliers and adders, and the memory size of LUT. Here, we consider N_s and N_h with 128 and 21 taps, R=2, k=5 and N=1024. Compared with the KK scheme, our proposed scheme can save the numbers of multipliers and adders by the factor of 7 and 29, respectively. While comparing with frequency-domain iterative scheme, the factors of multipliers and adders are 4 and 5.5, respectively. The memory sizes of these two iteration schemes are the same,

while nearly 2.7 times memory size is required for KK scheme.

V. Conclusion

In this paper, an iterative method with low complexity is proposed for minimum phase signal recovery without up-sampling in time domain. Based on the proposed scheme, the transmission of a 30GHz SSB 16-QAM DMT signal over 80km SMF with CD pre-compensation is successfully demonstrated with BER below hard-decision forward error correction (HD-FEC) threshold of 3.8×10^{-3}. The experimental results show that, our proposed scheme can achieve the same BER performance with frequency-domain iterative scheme and KK scheme. Since our proposed scheme is free from up-sampling and time-frequency domain conversion, the computational complexity can be reduced compared to KK receiver and frequency-domain iterative scheme. The proposed scheme can save the numbers of adders and multipliers by the factors of 29 and 7 compared with the KK scheme, while comparing with the frequency-domain iterative scheme, the factors are 5.5 and 4 for adders and multipliers, respectively. The experimental results show that our proposed scheme is a promising candidate in SSB DD system for 80km inter-DCIs.

References

[1] K. Zhong, X. Zhou, J. Huo, C. Yu, C. Lu, and A. P. T. Lau, "Digital Signal Processing for Short-Reach Optical Communications: A Review of Current Technologies and Future Trends," *J. Light. Technol*., vol. 36, no. 2, pp. 377-400, Jan. 2018.

[2] D. Zou, F. Li, Z. Li, W. Wang, Q. Sui, Z. Cao, and Z. Li, "100G PAM-6 and PAM-8 Signal Transmission Enabled by Pre-Chirping for 10-km Intra-DCI Utilizing MZM in C-band," *J. Light. Technol*., vol. 38, no. 13, pp. 3445-3453, Jul. 2020.

[3] J. Zhang, J. Yu, and H. Chien, "EML-based IM/DD 400G (4 × 112.5-Gbit/s) PAM-4 over 80 km SSMF Based on Linear Pre-Equalization and Nonlinear LUT Pre-Distortion for Inter-DCI Applications," in *Proc. Opt. Fiber Commun. Conf*., Los Angeles, CA, USA, 2017, Paper W4I.4.

[4] F. Devaux, Y. Sorel, and J. F. Kerdiles, "Simple Measurement of Fiber Dispersion and of Chirp Parameter of Intensity Modulated Light Emitter," *J. Light. Technol*., vol. 11, no. 12, pp. 1937-1940, Dec. 1993.

[5] B. Lin, J. Li, H. Yang, Y. Wan, Y. He, and Z. Chen, "Comparison of DSB and SSB Transmission for OFDM-PON," *J. Opt. Commun. Netw.*, vol. 4, no. 11, pp. 94-100, Nov. 2012.

[6] T. Bo, and H. Kim, "Generalized model of optical single sideband generation using dual modulation of DML and EAM," *Opt. Express*, vol. 28, no. 19, pp. 28491-28501, 2020.

[7] D. Lu, X. Zhou, J. Huo, J. Gao, Y. Yang, K. He, J. Yuan, K. Long, C. Yu, A. P. T. Lau, and C. Lu, "Theoretical CSPR Analysis and Performance Comparison for Four Single-Sideband Modulation Schemes With Kramers-Kronig Receiver," *IEEE Access*, vol 7, pp. 166257–166267, Oct. 2019.

[8] Z. Li, M. S. Erkılınc¸, K. Shi, E. Sillekens, L. Galdino, B. C. Thomsen, P. Bayvel, and R. I. Killey, "SSBI Mitigation and the Kramers-Kronig Scheme in Single-Sideband Direct-Detection Transmission with Receiver-Based Electronic Dispersion Compensation," *J. Light. Technol*., vol. 35, no. 10, pp. 1887-1893, May. 2017.

[9] W. R. Peng, I. Morita, and H. Tanaka, "Enabling high capacity direct-detection optical OFDM transmissions using beat interference cancellation receiver," in *Proc. 2010 Eur. Conf. Opt. Commun*., Sept. 2010, paper Tu.4.A.2.

[10] W. R. Peng, B. Zhang, K-M. Feng, X. Wu, A. E. Willner, and S. Chi, "Spectrally efficient direct-detected OFDM transmission incorporating a tunable frequency gap and an iterative detection technique," *J. Light. Technol*., vol. 27, no. 24, pp. 5723-5735, Dec. 2009.

[11] C. Sun, D. Che, and W. Shieh, "Comparison of Chromatic Dispersion Sensitivity between Kramers-Kronig and SSBI Iterative Cancellation Receiver," in *Proc. Opt. Fiber Commun. Conf*., San Diego, CA, USA, Mar. 2018, Paper W4E.4.

[12] D. Lu, Y. Yang, J. Gao, M. He, J. Huo, X. Zhou, and K. Long, "Comparison of SSBI Iterative Cancellation, Conventional KK and Up-sampling Free KK Receiver," *In Proc. ACP*, 2019, paper T1G.2..

[13] A. Mecozzi, C. Antonelli, and M. Shtaif, "Kramers-Kronig coherent receiver," *Optica*, vol. 3, no. 11, pp. 1220–1227, Nov. 2016.

[14] A. J. Lowery, T. Wang, and B. Corcoran, "Clipping-Enhanced Kramers-Kronig Receivers," in *Proc. Opt. Fiber Commun. Conf*., San Diego, CA, USA, Mar. 2019, Paper M1H.2.

[15] T. Bo, and H. Kim, "Performance Analysis of Kramers-Kronig Receiver in the Presence of IQ Imbalance," *IEEE Photon. Technol. Lett*., vol. 30, no. 24, pp. 2171-2174, Dec. 2018.

[16] S. An, Q. Zhu, J. Li, and Y. Su, "Modified KK Receiver with Accurate Field Reconstruction at Low CSPR condition," in *Proc. Opt. Fiber Commun. Conf*., San Diego, CA, USA, Mar. 2019, Paper M1H.3.

[17] T. Bo, and H. Kim, "Kramers-Kronig receiver operable without digital upsampling," *Opt. Express*, vol. 26, no. 11, pp. 13810-13818, 2018.

[18] T. Bo, and H. Kim, "Towards practical Kramers-Kronig receiver: Resampling, performance, and implementation," *J. Light. Technol*., vol. 37, no. 2, pp. 2194-2200, May. 2019.

[19] A. Mecozzi, "Retrieving the full optical response from amplitude data by Hilbert transform," *Optics Commun*., vol. 282, no. 20, pp. 4183-4187, 2009.

[20] A. Mecozzi, "A necessary and sufficient condition for minimum phase and implications for phase retrieval," *arXiv preprint* arXiv:1606.04861, 2016.

[21] R. W. Gerchberg and W. O. Saxton, "A practical algorithm for the determination of phase from image and diffraction plane pictures," *Optik*, vol. 35, no. 2, pp. 237-246, 1972.

[22] H. Zhou, K. Zou, P. Liao, A. Almaiman, F. Alishahi, A. Fallahpour, A. Minoofar, M. Tur and A. E. Willner, "WDM Operation and Multiple Dispersion Elements for a Direct-Detection System using Phase Retrieval," in *Proc. Opt. Fiber Commun. Conf*., San Diego, CA, USA, 2020, Paper W4A.4.

[23] R. K. Patel, I. A. Alimi, N. J. Muga, and A. N. Pinto, "Optical Signal Phase Retrieval with Low Complexity DC-Value Method," *J. Light. Technol*., vol. 38, no. 16, pp. 4205-4212, Aug. 2020.

[24] C. Füllner, M. M. H. Adib, S. Wolf, J. N. Kemal, W. Freude, C. Koos, and S. Randel, "Complexity Analysis of the Kramers-Kronig Receiver," *J. Light. Technol*., vol. 37, no. 17, pp. 4295-4307, Sep. 2019.

[25] T. Wang, and A. Lowery, "Minimum Phase Conditions in Kramers-Kronig Optical Receivers," *J. Light. Technol*., 2020, early access.

[26] C. Füllner, S. Wolf, J. N. Kemal, J. Lutz, L. Altenhain, R. Schmid, W. Freude, C. Koos, and S. Randel, "Transmission of 80-GBd 16-QAM over 300 km and Kramers-Kronig Reception Using a Low-Complexity FIR Hilbert Filter Approximation," in *Proc. Opt. Fiber Commun. Conf*., San Diego, CA, USA, 2018, Paper W4E.3.

[27] F. Li, D. Zou, L. Ding, Y. Sun, J. Li, Q. Sui, L. Li, X. Yi, and Z. Li, "100 Gbit/s PAM4 signal transmission and reception for 2-km interconnect with adaptive notch filter for narrowband interference," *Opt. Express*, vol. 26, no. 18, pp. 24066-24074, 2018.

[28] W. Wang, F. Li, Z. Li, Q. Sui, and Z. Li, "Dual-Drive Mach-Zehnder Modulator-Based Single Side-band Modulation Direct Detection System Without Signal-to-Signal Beating Interference," *J. Light. Technol*., vol. 38, no. 16, pp. 4341-4351, Aug. 2020.